HHS Public Access

Author manuscript

J Affect Disord. Author manuscript; available in PMC 2019 February 01.

Published in final edited form as:

J Affect Disord. 2018 February ; 227: 752–758. doi:10.1016/j.jad.2017.11.040.

A pilot resting-state functional connectivity study of the kynurenine pathway in adolescents with depression and healthy controls

Samuel J. DeWitt[a], **Kailyn A. Bradley**[a], **Na Lin**[b], **Chunli Yu**[b], and **Vilma Gabbay**[a,c]

[a]Department of Psychiatry, Icahn School of Medicine at Mount Sinai, New York, NY, USA

[b]Department of Genetics and Genomic Sciences Icahn School of Medicine at Mount Sinai, New York, NY, USA

[c]Nathan S. Kline Institute for Psychiatric Research, Orangeburg, NY, USA

Abstract

Background—The neuroimmunological kynurenine pathway (KP) has been hypothesized to play a role in depressive/anhedonic symptoms and related CNS disturbances. Indoleamine 2,3-dioxygenase (IDO) is the rate limiting enzyme which leads to neurotrophic [kynurenic acid (KA)] and neurotoxic [Quinolinic acid (QUIN)] branches. In this pilot, we sought to examine associations between blood KP neuro-toxic/trophic measures and anhedonia/depression associated networks in youth with major depression (MDD) and healthy controls (HC).

Methods—Subjects were 14 psychotropic-medication free adolescents with MDD and 7 HC, ages 12–19 yo. All underwent resting-state functional magnetic resonance imagining (fMRI) scans. Voxel-wise maps were generated indicating correlation strengths among 4 bilateral seeds [(dorsal anterior cingulate cortex (dACC), perigenual ACC (pgACC), subgenual ACC (sgACC) and nucleus accumbens (NAc)] and remaining brain regions. FMRI analyses were family-wise error corrected. KP metabolites were measured using liquid chromatography–tandem mass spectrometry.

Results—Connectivity between the right dACC and the right precuneus was positively correlated with KA levels. This same cluster demonstrated an inverse correlation with IDO activity. Exploratory analysis at a more liberal clustering threshold showed the KA/QUIN ratio was positively correlated with connectivity between the pgACC and the right medial prefrontal cortex. Lastly, connectivity between the pgACC and the left inferior temporal gyrus was positively correlated with QUIN levels.

Contributors

Samuel DeWitt analyzed data, and along with Kailyn Bradley, wrote the manuscript. Na Lin and Chunli Yu analyzed the KP data and assisted with manuscript preparation. Vilma Gabbay is the PI on the grant and was integral to all aspects of study design, data collection, analysis, and manuscript preparation. All authors have contributed to and have approved the final manuscript.

Conflicts of Interest

Conflicts of interest: none.

Limitations—Findings are preliminary due to the small sample size.

Conclusions—This pilot study is the first report in depressed adolescents demonstrating associations between the KP and anhedonia/depression-associated brain networks. This pilot adds evidence to the putative role of the KP in MDD.

Keywords

Kynurenine pathway; resting-state functional connectivity; adolescence; major depressive disorder; anhedonia

Introduction

Major depressive disorder (MDD) is highly prevalent in adolescence and poses a serious public health concern due to its deleterious outcomes, including increased suicide risk (Asarnow et al., 2008). Furthermore, adolescent MDD is a strong predictor of depression in adulthood (Weissman et al., 1999), which carries a high disability burden (Pine et al., 1999). As such, biological research of adolescent MDD, prior to chronicity effects, is of great importance. Considerable evidence suggests that activation of the immune system and the release of pro-inflammatory cytokines contribute to the development of major depression in adolescents and adults (Brundin et al., 2016; Gabbay et al., 2010). The kynurenine pathway (KP) has been hypothesized to play a key role in cytokine-induced depressive behaviors and related central nervous system (CNS) disturbances by the production of oxygen free radicals and highly potent neurotoxins (Amori et al., 2009; Schwarcz & Pellicciari, 2002). Indoleamine 2, 3-dioxygenase (IDO), the rate-limiting enzyme of the KP, is induced by pro-inflammatory cytokines and degrades tryptophan (TRP) into kynurenine (KYN) (Wirleitner et al., 2003). KYN is further metabolized into several neurotoxins, namely 3-hydroxykynurenine (3-HK) and 3-hydroxyanthranilic acid (3-HAA), whose downstream end product is quinolinic acid (QUIN), a glutamatergically-active N-methyl-D-aspartate (NMDA) receptor agonist. Alternately, KYN can also be metabolized into kynurenic acid (KA), a glutamate receptor antagonist, producing neuroprotective effects in the brain (Sapko et al., 2006). Converging data from preclinical and clinical work have implicated the KP in anhedonia, the reduced capacity to experience pleasure. Our laboratory previously documented increased IDO activity (indexed by the KYN/TRP ratio) in adolescents with MDD, but only in those with the melancholic subtype, characterized by anhedonia. We also reported positive associations between KP neurotoxins (KYN, 3-HAA) and increased striatal total choline (a marker for lipid peroxidation) in a group of adolescents with MDD with high levels of anhedonia (Gabbay et al., 2010). Similar findings linking KP activation to anhedonia/MDD symptomatology have also been reported in adults (Anderson et al., 1990; Cowen et al., 1989; Curzon & Bridges, 1970; Maes et al, 1996; Savitz et al., 2015d).

As anhedonia reflects deficits of reward processes (Hasler et al., 2004; Wacker et al., 2009), the above findings suggest the KP may play a role in impairing the neuronal reward circuitry. Relatedly, neuroimaging studies in adults with depression and bipolar disorder documented relationships between blood KP metabolite levels and reward-related brain regions. Findings include associations between IDO activity and striatal volume (Savitz et al., 2015a), KP neurotoxic metabolites and the medial PFC cortical thickness (Meier et al.,

2016), as well as amygdala and hippocampal volumes (Savitz et al., 2015b; Savitz et al., 2015c). Furthermore, ratios of neurotrophic to neurotoxic KP metabolites had distinct associations with hippocampal activation in participants with MDD compared to healthy controls (Young et al., 2016). One prior study also documented distinct associations between both the neurotoxic and neurotrophic branches of the KP and the perigenual anterior cingulate cortex (pgACC) network connectivity in a sample of adult football players with and without TBI and healthy controls (Meier et al., 2017). To the best of our knowledge, the latter reference represents the only resting state study of KP correlates, and there have not been any similar studies in youth or in individuals with depression or other psychiatric disorders.

In the present study, we sought to extend above observations and examine KP blood metabolite levels in relation to whole-brain intrinsic functional connectivity (iFC) of anhedonia-related regions in adolescents with MDD and heathy adolescents. These regions were established based on our prior resting-state functional magnetic resonance imaging (fMRI) study in adolescents with MDD that implicated striatal and salience/reward-related regions (i.e., dorsal anterior cingulate cortex (dACC) and subgenual anterior cingulate cortex (sgACC)) in anhedonic symptomatology (Gabbay et al., 2013). In addition, given previous findings that showed associations between the KP and pgACC connectivity in brain injury, and the significant role of this region in adolescent MDD (Rzepa & McCabe, 2016), we included the pgACC in the current investigation as well. We hypothesized that: 1) neurotrophic factors, such as KA and the KA/QUIN ratio would be associated with increased whole-brain iFC of our selected regions, demonstrating neuroprotection within the salience/reward network; and 2) conversely, QUIN levels and IDO activity (indexed by the KYN/TRP ratio) would be associated with decreased iFC due to network desegregation via excitotoxicity.

Methods

Study Participants

We studied 21 adolescents, 12–19 years old (mean age = 16.68, 15 female), 14 with MDD and 7 healthy controls (HC). Participants represent a subset of subjects from a previously published resting-state study (Gabbay et al., 2013) that had blood samples to be analyzed for KP metabolites. This study was approved by the appropriate Institutional Review Boards. Prior to beginning the study, procedures were explained to parents and participants. Participants 18 years of age or older provided consent, while those under 18 provided assent, and a parent or guardian provided consent.

Inclusion/Exclusion Criteria

Participants were excluded if they had any significant medical or neurological disorder, an IQ < 80, claustrophobia, or any MRI contraindication as assessed by a standard safety screening form. Additionally, a positive urine toxicology test, or a positive urine pregnancy test in females, on the day of the scan were exclusionary. All adolescents with MDD met the DSM-IV-TR criteria for MDD, with a current episode duration ≥ 6 weeks, a raw depression severity score ≥ 40 (T score > 63) on the Children's Depression Rating Scale–Revised

(CDRS-R) (Poznanski et al., 1985), and were psychotropic medication–free for at least 3 months. Exclusionary diagnoses for participants with MDD included a lifetime history of bipolar disorder, schizophrenia, pervasive developmental disorder, panic disorder, obsessive-compulsive disorder, conduct disorder, or Tourette's disorder. A substance use disorder in the past 12 months was also exclusionary. Lastly, a current diagnosis of posttraumatic stress disorder or an eating disorder were exclusionary. HC participants did not meet criteria for any current or past DSM-IV-TR diagnoses and had never been treated with psychotropic medication.

Imaging Data Acquisition

Imaging data were acquired on a 3.0 Tesla Siemens Allegra scanner as previously described in detail (Gabbay et al., 2013). The imaging protocol included a high-resolution T1-weighted magnetization prepared rapid acquisition gradient-echo [MPRAGE] sequence (repetition time [TR] = 2,500 ms; echo time [TE] = 3.93 ms; inversion time [TI] = 600 ms; flip angle = 8°; 176 slices; voxel size = 1×1×1 mm^3; field of view [FOV] = 256 × 256 mm^2) and a resting-state fMRI echo planar imaging (EPI) sequence (197 whole-brain volumes; TR = 2,000 ms; effective TE = 25 ms; flip angle = 90°; 39 contiguous 3-mm oblique axial slices parallel to the anterior commissure/posterior commissure line; voxel size = 3×3×3 mm^3; matrix = 64×64; FOV = 192×192 mm^2).

Imaging Data Analysis

Data were preprocessed using a combination of C-PAC (Craddock et al., 2013) and AFNI (NIMH Scientific and Statistical Computing Core, Bethesda, MD, US) tools. Preprocessing steps included slice time correction for interleaved slice acquisition, realignment by volume registration, mean-based intensity normalization, and bandpass filtering (0.01–0.1). High resolution anatomical images were transformed into Talairach (TLRC template space) using AFNI's @auto_tlrc, with functional images aligned to this transformed anatomical image using the @auto_tlrc linear resampling default option. This was followed by spatial smoothing using 3dBlurtoFWHM in AFNI with a 6mm full width at half maximum (FWHM) smoothing kernel.

The preprocessed data were regressed on 6 motion parameters. Frame-wise displacement was also calculated across all 197 frames. A scrubbing threshold of 2mm was used to indicate frames that demonstrated gross frame to frame motion. Resultant maps of scrubbed data did not differ in terms of surviving clusters compared to unscrubbed data; the results reported below include all 197 frames with the original 6 motion parameters regressed out. Seed based correlation maps were then generated and converted to MNI space for group level analysis using AFNI's 3dwarp-tta2mni option.

Bilateral seed regions of interest were selected based on our previous iFC study (Gabbay et al., 2013), including the dACC (±16, −6, 44), sgACC (±8, 10, 14), and the nucleus accumbens (NAc; (±9, 9 −8)). Additionally, although our previous study did not include a pgACC seed, this region has been implicated in reward function in adolescent MDD and was thus included here. We used coordinates (0, 38, 0) from a previous study that documented distinct pgACC connectivity patterns associated with decreased ability to anticipate pleasure

in adolescents at both high and low risk for depression (Rzepa & McCabe, 2016). Each seed region of interest (ROI) was a 3D sphere (volume = 268 × 1 mm^3 voxels, radius = 4mm) defined in MNI space.

Seed masks were applied to individual echo planar images (EPIs), and using the 3dfim+ command in AFNI, maps of the cross-correlation coefficients between the seed and every voxel in the brain were generated. CSF and white matter time series were derived using the AFNI 3dseg command to generate white matter and CSF masks thresholded at a 0.96 clip. CSF and white matter time series were regressed out during the generation of correlation maps. Using Fisher's Z-transformations, the correlation maps were converted to Z maps for group level analyses.

Random effects analyses were performed on Z maps at the group-level to identify surviving clusters per seed. Cluster thresholding and family-wise error (FWE) correction for multiple comparisons was applied using traditional 3dClustSim in AFNI. Residual images were derived from preprocessed resting-state images (following alignment to anatomical images in TLRC space) per person using the 3dDeconvolve function in AFNI. Smoothing parameters using 3dFWHMx were averaged across individuals (mean x y z: 6.59 6.42 6.35) and used for 3dClustSim. This estimates the probability of false positive activation clusters throughout the whole brain based on two criteria, smoothness of the voxel map and cluster-defining threshold. Effective smoothness (inherent smoothness plus smoothing applied) was estimated using individual residual images and averaged across the whole sample (the resulting smoothness was slightly over 6mm FWHM). We set the cluster-defining threshold to the 99.5th percentile of the t-statistic distribution. A FWE-corrected significance level of 0.05 yielded a required minimum cluster size of 41 voxels (at $p \leq 0.001$ uncorrected).

KP Methodology

TRP and other KP metabolites, including KA, KYN, QUIN, in plasma were measured by a liquid chromatography–tandem mass spectrometry (LC-MS/MS) method. IDO activity was indexed by the KYN/TRP ratio. Ethyl-4-hydroxy-2-quinolinecarboxylate was used as an internal standard. 100 μL plasma was pipetted into a 1.5 mL Eppendorf tube, and 300 μL acetonitrile and 10 μL 20 μM internal standard solutions were added and mixed. The mixture was vortexed for 10 sec and centrifuged at 16100 rcf for 5 min. The supernatant was transferred into a 96-well plate and dried under nitrogen at 40°C for 20 min. Samples were reconstituted with 50 μL of 5% acetonitrile for LC-MS/MS analysis.

An Agilent 6460 LC-MS/MS system was used for analysis in positive ESI mode. The capillary voltage was +3500 V and the nozzle voltage was +500 V. The ion source gas temperature was 300°C with a flow rate of 11 L/min. The sheath gas temperature was 150°C with a flow rate of 10 L/min. The nebulizer gas was 45 psi. Data were acquired by selected reaction monitoring (SRM) using specific transitions corresponding to TRP and KP metabolites. The optimal parameters for each compound are listed in Table 1.

Separation of TRP and KP metabolites was achieved using a Water Acquity HSS T3 column (100 mm × 2.1 mm internal diameter, 1.7 μm particle size) under gradient conditions with mobile phase A (0.5% formic acid in water) and mobile B (0.5% formic acid in acetonitrile).

The LC gradients started with 5% B, increased to 50% B from 2 to 13 min, increased to 100% B immediately, and kept 100% B from 13.1 to 14 min, followed by a decrease to 5% B from 14.1 min, and held until 24 min. The flow rate was 0.2 mL/min, and the injection volume was 2 μL. Six calibrators were used for generation of a calibration curve. The low limit of each compound was 0.125 μM for KA and KYN. Additionally, the low limit was 0.5 μM for QUIN and 2.5 μM for TRP.

Statistical Analyses

Statistical analyses were performed in SPSS, version 22. KP metabolites across the entire sample were not normally distributed, and thus non-parametric tests were used in all KP analyses. Mann-Whitney U-tests compared the metabolite levels of adolescents with MDD and HC adolescents. Spearman's rank order correlations assessed the relationship between average connectivity Z scores in surviving clusters that were extracted from the individual Z maps per seed region and KP metabolite levels. Furthermore, all connectivity and KP associations, as well as all connectivity maps, were examined in just the subset of the sample with MDD (N = 14). Lastly, in light of our small sample size, we performed exploratory analyses using clusters that survived at a more liberal threshold (uncorrected $p \leq 0.005$ $k \geq 89$) in order to examine all potential KP and connectivity associations.

Results

Demographic features

The subset of participants diagnosed with MDD consisted of 11 females and 3 males and had a mean age of 16.76 (SD = 3.04). The healthy controls consisted of 4 females and 3 males with a mean age of 16.53 (SD = 1.75). An independent samples t-test revealed no significant difference between the groups in age ($t(18) = 0.216$ $p = 0.831$, unequal variances assumed

KP metabolite levels

Concentration levels/ratios of the KP metabolites are listed in Table 2. There were no significant differences between adolescents with MDD and HC (all $p \geq 0.05$).

Seed-based resting-state functional connectivity (rsFC) (Whole sample)

All participants, MDD and HC, were included in the following seed-based group analyses. Independent samples t-tests revealed there were no significant differences in any of the head motion parameters between the MDD and HC groups (X direction, $t(7) = 0.64$,$p = 0.54$, unequal variances assumed; Y direction, $t(6)=0.90$ $p=0.40$, unequal variances assumed; Z direction, $t(19) = 0.16$, $p = 0.25$; Pitch, $t(6) = 0.73$, $p = 0.49$, unequal variances assumed; Roll, $t(7) = 0.84$, $p = 0.43$; Yaw, $t(19) = 0.21$, $p = 0.84$).

Surviving clusters by seed, separated by positive/negative connectivity, are displayed in Table 3; all results are thresholded at $p \leq 0.05$ (FWE corrected), cluster ≥ 42 voxels, unless noted as exploratory analyses. **Left dACC.** Clusters of significant positive connectivity were found in the right cingulate gyrus and left middle frontal gyrus. Clusters of significant negative connectivity were found in the right precuneus. **Right dACC.** One cluster of

significant positive connectivity was found in the left cingulate gyrus. Clusters of significant negative connectivity were found in the left/right precuneus. **sgACC.** No clusters survived thresholding for the right or left sgACC. **NAc.** No clusters survived thresholding for the right or left NAc. **pgACC.** One cluster of significant positive connectivity was found within the right hippocampus. Clusters of significant negative connectivity were found in the right precuneus and left inferior temporal gyrus (ITG).

Seed-Based rsFC (MDD group)

No new clusters were identified when looking at whole-brain connectivity within just the group of adolescents with MDD.

Correlations between KP metabolites and rsFC (Whole sample)

Right dACC-right precuneus connectivity was positively correlated with KA levels, $\rho = 0.44$, $p \leq 0.05$, see Figure 1A. The same cluster demonstrated an inverse correlation with IDO activity, $\rho = -0.65$ $p \leq 0.01$, see Figure 1B. No other rsFC values were significantly correlated with any other KP metabolites (all $p > .05$).

Correlations between KP metabolites and rsFC (MDD group)

When excluding the HC group, the inverse relationship between dACC-precuneus connectivity and IDO activity continued to be significant, at an even lower alpha level ($\rho = -0.77$ p 0.001). No other findings remained significant in the smaller sample of only adolescents with MDD.

Exploratory analyses (Whole sample)

Analyses were rerun using a more liberal FWE threshold ($p \leq 0.005$ uncorrected, $k > 89$). Results were still FWE corrected at $p \leq 0.05$. At this more liberal threshold, additional connections were significant with several seeds: **Left dACC:** There was an additional cluster of significant negative connectivity in the right middle temporal gyrus. **Right dACC:** There was an additional cluster of significant negative connectivity in the right middle temporal gyrus. **Left sgACC:** A cluster of positive connectivity with the left middle cingulate cortex was significant. **Left NAc:** A cluster of positive connectivity with the right pallidum/putamen was significant. **pgACC:** There were additional clusters of significant positive connectivity with the left middle temporal gyrus and the right medial frontal gyrus.

Additionally, there were clusters of significant negative connectivity with right superior parietal lobule, left middle frontal gyrus and left middle occipital gyrus. Additional KP-rsFC relationships were also found at this more liberal threshold. There was a positive correlation between pgACC-left ITG connectivity and QUIN levels, $\rho = 0.43$, $p \leq 0.05$ (Figure 1C). The ITG cluster location did not shift from the primary analyses, but the cluster size increased from 49 to 89 voxels. Additionally, there was a positive correlation between pgACC-right medial frontal gyrus connectivity and the KA/QUIN ratio, $\rho = 0.47$, $p \leq 0.05$ (Figure 1D). There were no additional findings when examining the MDD group alone.

Discussion

The present study is the first to document an association between the KP and iFC of salience/reward-related regions in a combined sample of adolescents with MDD and healthy adolescents. Findings confirmed our hypothesis that the neurotrophic branch of the KP would be associated with an increase in network connectivity, while the neurotoxic branch would be associated with a decrease. We documented that both the neurotrophic and neurotoxic branches of the KP are associated with distinct connectivity patterns between reward-related regions of the salience network to the default mode network (DMN). Specifically, we found that increased KA was associated with increased connectivity of the right dACC to the right precuneus, an important DMN hub. Furthermore, we showed that an increase in KA relative to QUIN (i.e., KA/QUIN ratio) was associated with increased connectivity between the pgACC and the medial prefrontal cortex (mPFC), another key DMN region. Meanwhile, IDO activity (indexed by the KYN/TRP ratio), previously linked to a worsening of depressive symptoms by way of the neurotoxic branch of the KP (Elovainio et al, 2012; Elovainio et al., 2011; Gabbay et al., 2012) was associated with decreased connectivity between the right dACC and the right precuneus. This finding remained significant when the HC sample was excluded from the analysis, and in fact was strengthened. This suggests that IDO activity may have a stronger association with network desegregation in those diagnosed with MDD. Interestingly, contrary to our initial hypothesis, increased neurotoxic QUIN levels were associated with increased connectivity between the pgACC and the left ITG. We discuss our findings below.

A major finding in this study was the positive correlation between the neurotrophic branch of the KP and connectivity of salience/reward network hubs (i.e., dACC and pgACC) with DMN hubs (i.e., precuneus and mPFC). The DMN consists of midline regions such as the mPFC, precuneus, and posterior cingulate cortex, and is shown to be more activated in the absence of goal-directed behavior (Biswal et al., 1997). A prevailing theory regarding the DMN is that its connectivity patterns serve as a blueprint for the brain and may inform goal-directed behavior (Kannurpatti et al., 2012). The salience network, made up of a combination of PFC and visual-spatial regions, identifies and evaluates internal and external cues worthy of attentional deployment (Uddin, 2017).

Our findings documented that the dACC and the right precuneus were inversely correlated with one another (i.e., demonstrated negative connectivity), with increased IDO activity associated with greater anticorrelation, while increased levels of KA were associated with increased correlation between the regions. As a DMN hub, the precuneus is primarily involved in self-referential processing (Kircher et al., 2000; Sajonz et al., 2010). Reduced inter-network connectivity of both the salience and DMN have previously been shown to be associated with worsening symptoms of depression (Servaas et al., 2017), and decreased precuneus/salience network connectivity has been reported in adolescents with depression compared to healthy controls (Sacchet et al., 2016). Meanwhile, shifts in self-referential processing towards negative rumination have been highlighted in depression (Nejad et al., 2013). Therefore, the finding of negative connectivity between these two regions in our study is most likely derived from the MDD group, which made up the majority of the sample. Our findings suggest that increased IDO activity may be associated with DMN/

salience disconnections, while the KP neurotrophic branch, via KA, may be associated with enhanced DMN/salience connectivity. This concept is supported by preclinical data demonstrating that peripheral inhibition of IDO has been shown to block its central transcription in the brain and subsequently block development of depressive-like behaviors following immunological stimulation (O'Connor et al., 2009; Salazar et al., 2012).

Our exploratory analyses further revealed a positive correlation between KA/QUIN and pgACC-mPFC positive connectivity, supporting the role of the neurotrophic branch of the KP in DMN/salience connectivity. Previous studies have shown peripheral inflammatory responses to be inversely correlated with medial PFC connectivity to the rest of the DMN (Marsland et al., 2017). It has been suggested that inflammatory responses affect cognitive control supported by subregions of the ACC and mPFC (Critchley & Harrison, 2013). Furthermore, evidence suggests the ratio of KA to neurotoxic metabolites mediates the relationship between MDD diagnosis and mPFC cortical thickness (Meier et al., 2016). Our present findings suggest that increased activation of the neurotrophic branch of the KP relative to the neurotoxic branch (i.e., KA/QUIN ratio levels) is associated with increased connectivity between these regions, which may potentially impact their functioning.

While our hypothesis that the neurotrophic branch of the KP would be associated with increased rsFC was supported, our prediction that the neurotoxic branch would show the opposite relationship was not. In fact, we found that increased QUIN levels were associated with increased connectivity between the pgACC and the left ITG. Though contrary to our predictions, this finding is not entirely surprising. Salience network connectivity (specifically the amygdala) to the temporal pole has previously been shown to be elevated in adolescents at high risk for MDD (Rzepa & McCabe). Indeed, both increases and decreases, particularly within the DMN, have been shown to be associated with MDD depending on the brain region, population of interest, and/or medication history (Rzepa & McCabe, 2016; Sacchet et al., 2016.). Therefore, our finding that QUIN levels were associated with increased connectivity patterns between the pgACC and the inferior temporal gyrus fits findings of increased salience network-temporal gyrus connectivity in MDD.

Limitations

While these findings document links between the KP and network connectivity, limitations should be noted. The main concern is the small sample size, which introduces type I and II errors. Further, there was an imbalance between individuals with and without MDD in the entire sample. Coupled with the small sample size, this makes it difficult to determine how much our findings were driven by those participants diagnosed with MDD. Also, given our small sample size and the exploratory nature of this study, our cluster threshold was determined using AFNI's traditional 3dClustSim method, rather than the updated autocorrelation function (ACF), which reports more conservative cluster thresholds. Lastly, despite previous evidence of links between the KP and striatum, our findings did not demonstrate any associations between the KP and NAc connectivity. Given that previous findings were reported in clinical samples, the heterogeneity of our sample, along with its small size, may be the reason for the lack of NAc findings.

Conclusion

This pilot study provides additional data for the possible effects of the inflammatory kynurenine pathway on brain function. These findings suggest that activation of the KP is associated with distinct alterations in connectivity of DMN/salience regions. Future studies are needed in larger samples of depressed adolescents in order to identify more specific associations between symptom severity and neuroinflammatory-connectivity interactions.

Acknowledgments

We would like to thank Michael Milham, M.D., Ph.D. for his help with the resting-state preprocessing pipeline.

Funding Statement

This study was supported by grants from the National Institute of Mental Health (NIMH) to Vilma Gabbay (grant numbers MH095807, MH101479). The content is solely the responsibility of the authors and does not necessarily represent the views of the NIMH. The NIMH had no further role in the design, collection of data, management, analysis, interpretation of data, or preparation of the manuscript.

References

Amori L, Guidetti P, Pellicciari R, Kajii Y, Schwarcz R. On the relationship between the two branches of the kynurenine pathway in the rat brain in vivo. Journal of neurochemistry. 2009; 109:316–325. [PubMed: 19226371]

Anderson IM, Parry-Billings M, Newsholme EA, Poortmans JR, Cowen PJ, et al. Decreased plasma tryptophan concentration in major depression: relationship to melancholia and weight loss. Journal of affective disorders. 1990; 20:185–191. [PubMed: 2148339]

Asarnow JR, Baraff LJ, Berk M, Grob C, Devich-Navarro M, Suddath R, Piacentini J, Tang L. Pediatric emergency department suicidal patients: two-site evaluation of suicide ideators, single attempters, and repeat attempters. Journal of the American Academy of Child and Adolescent Psychiatry. 2008; 47:958–966. [PubMed: 18596552]

Biswal BB, Van Kylen J, Hyde JS. Simultaneous assessment of flow and BOLD signals in resting-state functional connectivity maps. NMR in biomedicine. 1997; 10:165–170. [PubMed: 9430343]

Brundin L, Sellgren CM, Lim CK, Grit J, Palsson E, Landen M, Samuelsson M, Lundgren K, Brundin P, Fuchs D, Postolache TT, Traskman-Bendz L, Guillemin GJ, Erhardt S. An enzyme in the kynurenine pathway that governs vulnerability to suicidal behavior by regulating excitotoxicity and neuroinflammation. Translational psychiatry. 2016; 6:e865. [PubMed: 27483383]

Cowen PJ, Parry-Billings M, Newsholme EA, et al. Decreased plasma tryptophan levels in major depression. Journal of affective disorders. 1989; 16:27–31. [PubMed: 2521647]

Craddock C, Sikka S, Cheung B, Khanuja R, Ghosh SS, Yan C, Li Q, Lurie D, Vogelstein J, Burns R, Colcombe S, Mennes M, Kelly C, Di Martino A, Castellanos FX, Milham M. Towards Automated Analysis of Connectomes: The Configurable Pipeline for the Analysis of Connectomes (C-PAC). Frontiers in Neuroinformatics. 2013

Critchley HD, Harrison NA. Visceral influences on brain and behavior. Neuron. 2013; 77:624–638. [PubMed: 23439117]

Curzon &, Bridges GB, PK. Tryptophan metabolism in depression. Journal of Neurology, Neurosurgery and Psychiatry. 1970; 33:698–704.

Elovainio M, Hurme M, Jokela M, Pulkki-Raback L, Kivimaki M, Hintsanen M, Hintsa T, Lehtimaki T, Viikari J, Raitakari OT, Keltikangas-Jarvinen L. Moderating effect of indoleamine 2,3-dioxygenase (IDO) activation in the association between depressive symptoms and carotid atherosclerosis: evidence from the Young Finns study. Journal of affective disorders. 2011; 133:611–614. [PubMed: 21600662]

Elovainio M, Hurme M, Jokela M, Pulkki-Raback L, Kivimaki M, Hintsanen M, Hintsa T, Lehtimaki T, Viikari J, Raitakari OT, Keltikangas-Jarvinen L. Indoleamine 2,3-dioxygenase activation and

depressive symptoms: results from the Young Finns Study. Psychosomatic Medicine. 2012; 74:675–681. [PubMed: 22929065]

Gabbay V, Ely BA, Babb J, Liebes L. The possible role of the kynurenine pathway in anhedonia in adolescents. J Neural Transm (Vienna). 2012; 119:253–260. [PubMed: 21786117]

Gabbay V, Ely BA, Li Q, Bangaru SD, Panzer AM, Alonso CM, Castellanos FX, Milham MP. Striatum-based circuitry of adolescent depression and anhedonia. Journal of the American Academy of Child and Adolescent Psychiatry. 2013; 52:628–641. e613. [PubMed: 23702452]

Gabbay V, Klein RG, Katz Y, Mendoza S, Guttman LE, Alonso CM, Babb JS, Hirsch GS, Liebes L. The possible role of the kynurenine pathway in adolescent depression with melancholic features. Journal of child psychology and psychiatry, and allied disciplines. 2010; 51:935–943.

Hasler G, Drevets WC, Manji HK, Charney DS. Discovering Endophenotypes for Major Depression. Neuropsychopharmacology. 2004; 29:1765–1781. [PubMed: 15213704]

Kannurpatti SS, Rypma B, Biswal BB. Prediction of Task-Related BOLD fMRI with Amplitude Signatures of Resting-State fMRI. Frontiers in systems neuroscience. 2012; 6:7. [PubMed: 22408609]

Kircher TTJ, Senior C, Phillips ML, Benson PJ, Bullmore ET, Brammer M, Simmons A, Williams SCR, Bartels M, David AS. Towards a functional neuroanatomy of self processing: effects of faces and words. Cognitive Brain Research. 2000; 10:133–144. [PubMed: 10978701]

Maes M, Wauters A, Verkerk R, Ing RT, Demedts P, Neeels H, Van Gastel A, Cosyns P, Scharpe S, Desnyder R, et al. Lower Serum L-Tryptophan Availability in Depression as a Marker of a More Generalized Disorder in Protein Metabolism. Neuropsychopharmacology. 1996; 15:243–251. [PubMed: 8873107]

Marsland AL, Kuan DC, Sheu LK, Krajina K, Kraynak TE, Manuck SB, Gianaros PJ. Systemic inflammation and resting state connectivity of the default mode network. Brain, behavior, and immunity. 2017; 62:162–170.

Meier TB, Lancaster MA, Mayer AR, Teague TK, Savitz J, et al. Abnormalities in Functional Connectivity in Collegiate Football Athletes with and without a Concussion History: Implications and Role of Neuroactive Kynurenine Pathway Metabolites. Journal of neurotrauma. 2017; 34:824–837. [PubMed: 27618518]

Meier TB, Drevets WC, Wurfel BE, Ford BN, Morris HM, Victor TA, Bodurka J, Teague TK, Dantzer R, Savitz J. Relationship between neurotoxic kynurenine metabolites and reductions in right medial prefrontal cortical thickness in major depressive disorder. Brain, behavior, and immunity. 2016; 53:39–48.

Nejad AB, Fossati P, Lemogne C. Self-referential processing, rumination, and cortical midline structures in major depression. Frontiers in human neuroscience. 2013; 7:666. [PubMed: 24124416]

O'Connor JC, Lawson MA, Andre C, Moreau M, Lestage J, Castanon N, Kelley KW, Dantzer R. Lipopolysaccharide-induced depressive-like behavior is mediated by indoleamine 2,3-dioxygenase activation in mice. Molecular psychiatry. 2009; 14:511–522. [PubMed: 18195714]

Pine DS, Cohen E, Cohen P, Brook J. Adolescent Depressive Symptoms as Predictors of Adult Depression: Moodiness or Mood Disorder? The American Journal of Psychiatry. 1999; 156:133–135. [PubMed: 9892310]

Poznanski EO, Freeman LN, Mokros HB, et al. Children's Depression Rating Scale - Revised. Psychopharmacology Bulletin. 1985; 21:979–989.

Rzepa E, McCabe C. Decreased anticipated pleasure correlates with increased salience network resting state functional connectivity in adolescents with depressive symptomatology. Journal of psychiatric research. 2016; 82:40–47. [PubMed: 27459031]

Sacchet MD, Ho TC, Connolly CG, Tymofiyeva O, Lewinn KZ, Han LK, Blom EH, Tapert SF, Max JE, Frank GK, Paulus MP, Simmons AN, Gotlib IH, Yang TT. Large-Scale Hypoconnectivity Between Resting-State Functional Networks in Unmedicated Adolescent Major Depressive Disorder. Neuropsychopharmacology. 2016; 41:2951–2960. [PubMed: 27238621]

Sajonz B, Kahnt T, Margulies DS, Park SQ, Wittmann A, Stoy M, Strohle A, Heinz A, Northoff G, Bermpohl F. Delineating self-referential processing from episodic memory retrieval: common and dissociable networks. NeuroImage. 2010; 50:1606–1617. [PubMed: 20123026]

Salazar A, Gonzalez-Rivera BL, Redus L, Parrott JM, O'Connor JC. Indoleamine 2,3-dioxygenase mediates anhedonia and anxiety-like behaviors caused by peripheral lipopolysaccharide immune challenge. Hormones and behavior. 2012; 62:202–209. [PubMed: 22504306]

Sapko MT, Guidetti P, Yu P, Tagle DA, Pellicciari R, Schwarcz R. Endogenous kynurenate controls the vulnerability of striatal neurons to quinolinate: Implications for Huntington's disease. Experimental neurology. 2006; 197:31–40. [PubMed: 16099455]

Savitz J, Dantzer R, Meier TB, Wurfel BE, Victor TA, McIntosh SA, Ford BN, Morris HM, Bodurka J, Teague TK, Drevets WC. Activation of the kynurenine pathway is associated with striatal volume in major depressive disorder. Psychoneuroendocrinology. 2015a; 62:54–58. [PubMed: 26232650]

Savitz J, Dantzer R, Wurfel BE, Victor TA, Ford BN, Bodurka J, Bellgowan PS, Teague TK, Drevets WC. Neuroprotective kynurenine metabolite indices are abnormally reduced and positively associated with hippocampal and amygdalar volume in bipolar disorder. Psychoneuroendocrinology. 2015b; 52:200–211. [PubMed: 25486577]

Savitz J, Drevets WC, Smith CM, Victor TA, Wurfel BE, Bellgowan PS, Bodurka J, Teague TK, Dantzer R. Putative neuroprotective and neurotoxic kynurenine pathway metabolites are associated with hippocampal and amygdalar volumes in subjects with major depressive disorder. Neuropsychopharmacology. 2015c; 40:463–471. [PubMed: 25074636]

Savitz J, Drevets WC, Wurfel BE, Ford BN, Bellgowan PS, Victor TA, Bodurka J, Teague TK, Dantzer R. Reduction of kynurenic acid to quinolinic acid ratio in both the depressed and remitted phases of major depressive disorder. Brain, behavior, and immunity. 2015d; 46:55–59.

Schwarcz R, Pellicciari R. Manipulation of brain kynurenines: glial targets, neuronal effects, and clinical opportunities. The Journal of pharmacology and experimental therapeutics. 2002; 303:1–10. [PubMed: 12235226]

Servaas MN, Riese H, Renken RJ, Wichers M, Bastiaansen JA, Figueroa CA, Geugies H, Mocking RJ, Geerligs L, Marsman JB, Aleman A, Schene AH, Schoevers RA, Ruhe HG. Associations between Daily Affective Instability and Connectomics in Functional Subnetworks in Remitted Patients with Recurrent Major Depressive Disorder. Neuropsychopharmacology. 2017

Uddin LQ. What Is Salience?. 2017:1–4.

Wacker J, Dillon DG, Pizzagalli DA. The role of the nucleus accumbens and rostral anterior cingulate cortex in anhedonia: integration of resting EEG, fMRI, and volumetric techniques. NeuroImage. 2009; 46:327–337. [PubMed: 19457367]

Weissman MM, Wolk S, Goldstein RB, Moreau D, Adams P, Greenwald S, Klier CM, Ryan ND, Dahl RE, Wickramaratne P. Depressed Adolescents Grown Up. Journal of the American Medical Association. 1999; 281:1707–1713. [PubMed: 10328070]

Wirleitner B, Neurauter G, Schrocksnadel K, Frick B, Fuchs D. Interferon-gamma-induced conversion of tryptophan: immunologic and neuropsychiatric aspects. Current Medicinal Chemistry. 2003:1581–1591. [PubMed: 12871129]

Young KD, Drevets WC, Dantzer R, Teague TK, Bodurka J, Savitz J. Kynurenine pathway metabolites are associated with hippocampal activity during autobiographical memory recall in patients with depression. Brain, behavior, and immunity. 2016; 56:335–342.

Highlights

- Neurotrophic Kynurenine pathway (KP) metabolites (Kynurenic acid (KA), KA/quinolinic acid ratio) are associated with increased salience/default mode network (DMN) connectivity.
- Indoleamine 2, 3-dioxygenase, the rate limiting enzyme for the KP, is associated with decreased salience/DMN connectivity.
- Increase in neurotoxic quinolinic acid is associated with increased connectivity of the perigenual anterior cingulate cortex (pgACC) to the inferior temporal gyrus.

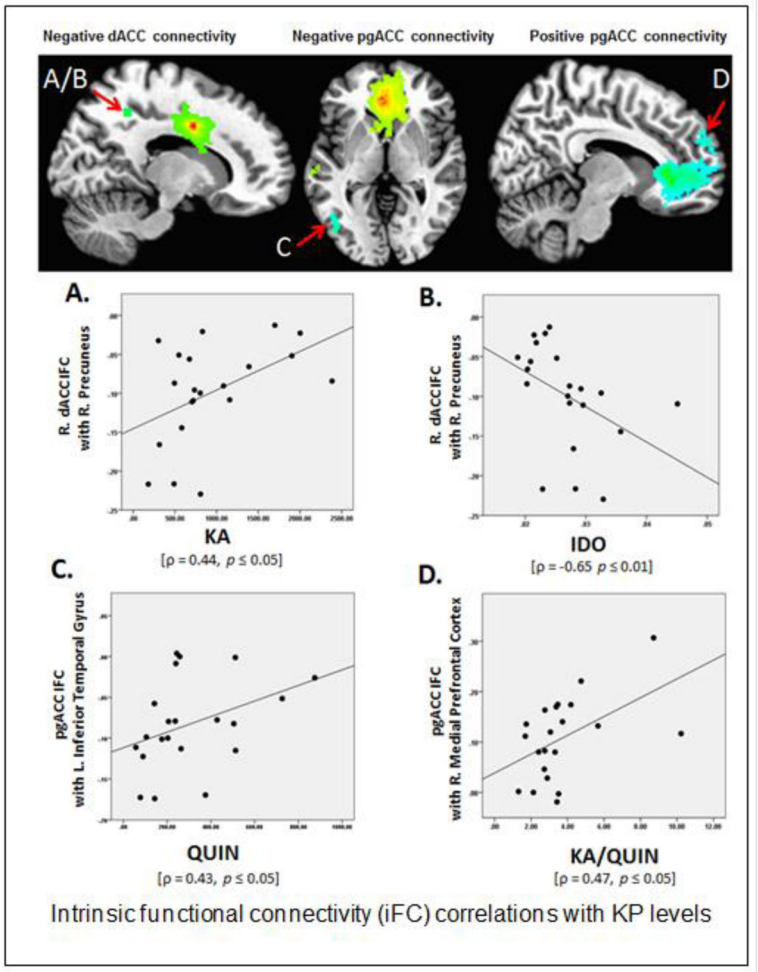

Figure 1.

Intrinsic functional connectivity (iFC) correlations with KP levels **A.** Right dACC negative iFC with the right precuneus demonstrated a positive correlation with KA levels, $\rho = 0.44$, $p \leq 0.05$. **B.** Right dACC negative iFC with right precuneus demonstrated a negative correlation with IDO activity (indexed by the KYN/TRP ratio), $\rho = -0.65$ $p \leq 0.01$. **C.** pgACC negative iFC with the left inferior temporal gyrus demonstrated a positive correlation with QUIN levels, $\rho = 0.43$, $p \leq 0.05$. **D**. pgACC positive iFC with the right medial prefrontal cortex demonstrated a positive correlation with KA/QUIN ratio, $\rho = 0.47$, $p \leq 0.05$. All maps FWE corrected at $p \leq 0.05$. A/B map thresholded at $p \leq 0.001$ uncorrected $K \geq 42$. C/D maps at $p \leq 0.005$ uncorrected $K \geq 89$

Table 1

Optimal parameters of compounds

Compound	Precursor	Product	Frag (V)	CE (V)
Kynurenine	209.1	192	72	4
Tryptophan	205.1	188	72	4
Kynurenic acid	190.1	144	92	20
Quinolinic acid	168.1	78	80	24

Table 2

Mean (SD) plasma concentrations of indoleamine 2,3-dioxygenase (IDO; indexed by the KYN/TRP ratio) kynurenic acid (KA), quinolinic acid (QUIN) (nM/L) and the KA/QUIN ratio in adolescents with MDD and healthy controls (HC).

Measure	**MDD *(N=14)***	**HC *(N=7)***
IDO activity (KYN/TRP)	0.028 (0.01)	0.02 (0.002)
KA	887.38 (382.94)	1053.96 (937.24)
QUIN	263.00 (143.34)	384.32 (320.90)
KA/QUIN	4.22 (2.47)	2.67 (0.85)

J Affect Disord. Author manuscript; available in PMC 2019 February 01.

Table 3

Intrinsic functional connectivity (iFC) clusters by seed region ($P \leq 0.05$ FWE corrected clusters ≥ 41 voxels, unless otherwise specified.)

			(MNI)			
Seed Region	**Connectivity Peak**	**Cluster Size(#voxels)**	**X**	**Y**	**Z**	**Valence (+/−)**
Right dACC	Left cingulate gyrus	153	−18	4	44	+
	Right precuneus	49	12	−50	50	−
	Left precuneus	42	−12	−62	44	−
	Right precuneus	42	2	−78	58	−
	Right middle temporal gyrus*	137	32	−62	26	−
Left dACC	Right precuneus	108	26	−54	24	−
	Right precuneus	77	20	−58	46	−
	Right cingulate gyrus	66	26	−2	30	+
	Left middle frontal gyrus	56	−24	16	34	+
	Right cingulate gyrus	54	12	−4	36	+
	Right middle temporal gyrus*	139	42	−54	16	−
Left sgACC	Left middle cingulate cortex*	132	0	−12	36	+
pgACC	Right precuneus	164	2	−80	48	−
	Right hippocampus	56	26	−12	−14	+
	Left inferior temporal gyrus	49	−46	−66	−2	−
	Right superior parietal lobule*	177	28	−70	54	−
	Left middle temporal gyrus*	152	−56	−16	−8	+
	Right MFG*	114	8	60	22	+
	Left middle frontal gyrus*	109	−44	38	26	−
	Left middle occipital gyrus*	104	−26	−82	24	−
Left NAc	Right pallidum/putamen	102	24	−2	4	−